Loss-of-function mutations in ADCY3 cause monogenic severe obesity

S. Saeed, A. Bonnefond, F. Tamanini, M. U. Mirza, J. Manzoor, Q. M. Janjua, S. M. Din, J. Gaitan, A. Milochau, E. Durand, et al.

Loss-of-function mutations in *ADCY3* cause monogenic severe obesity

Sadia Saeed[1,2], Amélie Bonnefond[1], Filippo Tamanini[2], Muhammad Usman Mirza[3], Jaida Manzoor[4], Qasim M. Janjua[5], Sadia M. Din[6], Julien Gaitan[7,8], Alexandra Milochau[7,8], Emmanuelle Durand[1], Emmanuel Vaillant[1], Attiya Haseeb[6], Franck De Graeve[1], Iandry Rabearivelo[1], Olivier Sand[1], Gurvan Queniat[1], Raphaël Boutry[1], Dina A Schott[9], Hina Ayesha[10], Muhammad Ali[11], Waqas I. Khan[12], Taeed A. Butt[13], Tuula Rinne[14], Connie Stumpel[15], Amar Abderrahmani[1,2], Jochen Lang[7,8], Muhammad Arslan[5,6] and Philippe Froguel[1,2]

[1]University of Lille, CNRS, Institut Pasteur de Lille, UMR 8199 – EGID, Lille, 59000, France; [2]Department of Genomics of Common Disease, Imperial College London, London, UK; [3]Department of Pharmaceutical and Pharmacological Sciences, Rega Institute for Medical Research, KU Leuven (University of Leuven), Leuven, Belgium; [4]Department of Paediatric Endocrinology, Children's Hospital, Lahore, Pakistan; [5]Centre for Research in Molecular Medicine, The University of Lahore, Lahore, Pakistan; [6]Department of Biological Sciences, Forman Christian College, Lahore, Pakistan; [7]Laboratory of Membrane Chemistry and Biology (CBMN), CNRS UMR 5248, Université de Bordeaux, France; [8]Université de Bordeaux, 351 Cours de la Libération, Talence, France; [9]Department of Pediatrics, Zuyderland Hospital, Heerlen, the Netherlands; [10]Department of Paediatrics, Punjab Medical College, Faisalabad, Pakistan; [11]Department of Paediatrics, Mayo Hospital, King Edward Medical University, Lahore, Pakistan; [12]Children Hospital and Institute of Child Health, Multan, Pakistan;[13]Department of Paediatrics, Fatima Memorial Hospital, Lahore, Pakistan; [14]Department of Human Genetics, Donders Centre for Neuroscience, Radboud University Medical Center, Nijmegen, The Netherlands; [15]Department of Clinical Genetics and GROW-School for Oncology and Developmental Biology, Maastricht University Medical Center, The Netherlands.

Study of monogenic forms of obesity have demonstrated the pivotal role of the central leptin-melanocortin pathway in controlling energy balance, appetite and body weight[1]. So far, the majority of loss-of-function mutations (mostly recessive or co-dominant) have been identified in genes that are directly involved in the leptin-melanocortin signalling. These genes, however, only explain obesity in <5% of cases, predominantly from outbred populations[2]. We previously show that in a consanguineous population of Pakistan, recessive mutations in known obesity genes explain ~30% of cases with severe obesity[3-5]. These data suggested that novel monogenic forms of obesity could also be identified in this population. Here we identify and functionally characterize homozygous mutations in the gene encoding adenylate cyclase 3 (ADCY3*)* in children with severe obesity, from consanguineous Pakistani families, and compound heterozygous mutations in a severely obese European/American child. These findings highlight ADCY3 as an important mediator of energy homeostasis and an attractive pharmacological target in obesity treatment.

Obesity with its complications has emerged as a major contributor to the global health burden and assumed the status of a pandemic[6]. At least 2.8 million people die each year as a consequence of being overweight or obese[7]. Although obesity is one of the most heritable diseases[8], the genetic etiology of a large proportion of obesity cases remains elusive.

Here, we performed whole exome sequencing (WES) in 138 probands presenting severe, early-onset obesity (BMI SDS ≥3) and their available family members (n= 117) from consanguineous families from the Punjab province of Pakistan. Through successive filtration steps **(Fig. 1a),** we identified four severely obese children from three unrelated families **(Fig. 1b: Family 1, 2, 3; Supplementary Fig. 1**) carrying novel or extremely rare homozygous mutations in *ADCY3* (NM_004036.4). The three potentially causative mutations included a frameshift mutation, c.3315del; p.Ile1106Serfs*3 (*mutADCY3*-I), a splice-site mutation, c.2578-1G>A (*mutADCY3*-II) and a non-synonymous missense mutation, c.191A>T, p.Asn64Ile (*mutADCY3*-III) (**Fig. 1b,1c; Supplementary Fig. 2**). Both *mutADCY3*-I and *mutADCY3*-II variants were novel and were not present in the Exome Aggregation Consortium (ExAC), the Single Nucleotide Polymorphism Database (dbSNP) or the Exome Sequencing Project (EPS). The splice-site *mutADCY3*-II was predicted to abolish the splice-acceptor-site **(Supplementary Note 1)**. The *mutADCY3*-III (rs541941351) is documented in ExAC with a global frequency of 3×10^{-4}. This missense mutation is predicted to be deleterious according to PolyPhen. All parents were heterozygous carriers of the respective *ADCY3* mutations (**Fig. 1b, Supplementary Table 2**). *ADCY3* was found within a large region of homozygosity (30-68 Mb) shared by affected subjects (data not shown).

Importantly, our filtration process did not report recessive variants in any other putative gene causing monogenic obesity **(Fig. 1a)**.

In a separate and independent investigation, WES identified a compound heterozygous *ADCY3* mutation in a child with severe obesity, from a non-consanguineous European/American family **(Fig. 1b: Family 4; Supplementary Fig. 1**). This compound heterozygous mutation included a frameshift mutation, c.1268del, p.Gly423Alafs*19 (*mutADCY3*-IVa) and an amino acid deletion, c.3354_3356del, p.Phe1118del (*mutADCY3*-IVb) (**Fig. 1c, Supplementary Fig. 2**). The *mutADCY3*-IVa was novel whereas *mutADCY3*-IVb (rs750852737) is documented in ExAC with a global frequency of 4×10^{-5}. The *mutADCY3*-IVa and *mutADCY3*-IVb were paternally and maternally inherited, respectively (**Supplementary Fig. 2)**. All *ADCY3* mutation sites are highly conserved across various species suggesting their evolutionary significance **(Supplementary Fig. 3)**.

ADCY3 is a member of a family of ten closely related cyclases that catalyse the synthesis of 3',5'-cyclic adenosine monophosphate (cAMP) from adenosine triphosphate (ATP), of which nine are anchored to the plasma membrane. We first assessed the dynamic and structural consequences of the mutations on ATP binding. Homology modelling followed by molecular dynamic (MD) simulations was performed to investigate conformational changes in terms of the root-mean-square deviation (RMSD). Structural analysis was possible only for *mut*ADCY3-I and *mut*ADCY3-II, where the crystal structures of the relevant ADCY3 domains were available. The mutated structures destabilized the backbone atoms resulting in partial unfolding of the catalytic domains. These changes in the mutated proteins displaced ATP from the binding site whereas the wild-type protein remained stable for the entire simulation period **(Fig. 2a)**. Residual flexibility profile of each of the two proteins indicated higher fluctuations (RMSF) compared to the wild-type **(Fig. 2b)**, thus predicting inability of the mutated protein to bind to ATP. Details of homology modelling and MD simulation are available in **Supplementary Note 2**. We, therefore, hypothesize that these mutations destabilize the ADCY3 catalytic domains resulting in a loss of protein function.

To further test this hypothesis, we transiently over-expressed the recombinant Myc-tagged, wild-type ADCY3 (Myc-hADCY3-wt) and each of the four mutant proteins (Myc-hADCY3-mut: *mut*ADCY3-I, *mut*ADCY3-II, *mut*ADCY3-III and *mut*ADCY3-IVb) in baby hamster kidney (BHK) cells. The protein expression and cellular localization of the wild-type and mutant ADCY3 were equivalent, as monitored by Western blotting and immunofluorescence **(Supplementary**

Fig. 4 and 5). Also, transient expression of either wild-type or each mutant ADCY3 did not significantly alter basal cAMP levels compared to the control plasmid (**Supplementary Fig. 4).** Stimulation of adenylate cyclase activity with forskolin and concomitant inhibition of endogenous phosphodiesterases with 3-isobutyl-1-methylxanthine (IBMX) led to a significantly higher increase in cAMP levels in cells over-expressing wild-type ADCY3 as well as *mut*ADCY3-III (~50-fold) compared to control and *mut*ADCY3-I, *mut*ADCY3-II and *mut*ADCY3-IVb transfected cells (~25-fold increase) (**Fig. 2c**). These data strongly support that *mut*ADCY3-I, *mut*ADCY3-II and *mut*ADCY3-IVb, affect the ADCY3 catalytic activity whereas the *mut*ADCY3-III does not. Similar results were found through luciferase assays: the stimulatory effect of *mut*ADCY3-I, *mut*ADCY3-II and *mut*ADCY3-IVb on the activity of cAMP responsive element (CRE-Luc) in response to IBMX and Forskolin was significantly lower (9-, 7- and 9-fold increase, respectively) compared to hADCY3-wt and *mut*ADCY3-III (attaining 13- and 11-fold increase, respectively; **Supplementary Fig. 6**). Interestingly, the expression level of *ADCY3* mRNA in white blood cells of Family 1 for which mRNA was available, was normal in the affected homozygous child with *mut*ADCY3-I, compared to his unaffected heterozygote sibling (**Supplementary Fig. 7**).

Taken together these data imply that *mut*ADCY3-I, *mut*ADCY3-II and *mut*ADCY3-IVb are loss-of-function mutations that dramatically and directly affect the catalytic activity and thereby cAMP production. The *mut*ADCY3-III that failed to alter ADCY3 catalytic activity is located in the globular cytosolic N-terminal domain and involves a substitution of a small polar amino acid to a large hydrophobic one that likely restricts the protein conformation. This suggests that *mut*ADCY3-III might lead to impaired ADCY3 function and thereby promote obesity in the affected patient via impaired G protein-coupled receptor interactions. Overall, our genetic and functional data support the identification of a novel form of monogenic obesity associated with mutations in *ADCY3,* which result, with the exception of *mut*ADCY3-III, in the defective catalytic activity and cAMP production.

Consistent with our observations of subjects with *ADCY3* mutations **(Table 1, Supplementary Table 1 and Fig. 1)**, *Adcy3*$^{-/-}$ mice are hyperphagic and obese[9]. Hyperphagia in the probands was first reported between 0.5-2 years of age. The wild-type or heterozygous family members presented normal body weight except parents of proband 2 (P2), that reportedly were accustomed to fat and carbohydrate enriched food (**Supplementary Table 2)**. Interestingly, the three probands P1, P3 and P4 were anosmatic when clinically tested, an observation that is in agreement with findings in *Adcy3*$^{-/-}$ mice[10]. The sense of smell was, however, only slightly abnormal in P2 and his

affected cousin. Although no quantitative data are available on physical activity, the two affected patients (P1 and P3) had slight-to-moderate intellectual disability despite normal body growth whereas probands P2 and P4 had normal intellect. No dysmorphic features were observed. The only affected female (P1), the oldest of the four probands, had menarche at 14 years but had no subsequent menstrual cycles. In this subject, obesity appeared more severe compared to the younger probands, and was accompanied by hyperlipidemia, hyperleptinemia and insulin resistance **(Table 1, Supplementary Table 1)**. These observations are also consistent with those of *Adcy3*$^{-/-}$ mice exhibiting an age-related increase in adiposity[9].

ADCY3 is expressed in the hypothalamus and selective ablation of *Adcy3* in the mouse hypothalamus results in a significant increase in body-fat mass[11]. Conversely, mice with a gain-of-function mutation in *Adcy3* have less fat compared to wild-type animals and are resistant to obesity when fed a high-fat diet[12]. ADCY3 is known to mediate the action of hormones involved in energy, lipid and glucose control[13]. Anorexigenic gut peptides such as GLP-1 that utilise G-protein coupled receptors for signalling, act centrally to control appetite by up-regulating ADCY3-mediated cAMP production[14]. Moreover, the anti-diabetic drug liraglutide (a GLP-I agonist) enhances expression of *Adcy3* at mRNA and protein levels[15], resulting in a weight reducing effect through its direct effect on the hypothalamus[16]. This suggests that *ADCY3* pathogenic mutations interfere with several anorexigenic-signaling cascades. Furthermore, ADCY3-cAMP signaling also regulates the proliferation and differentiation of adipocytes and intracellular processes related to adipogenesis and lipolysis[17]. *Adcy3* haploinsufficient (*Adcy3*$^{-/+}$) mice exhibit increased adipogenesis and adiposity without hyperphagia[18]. Therefore, a potent peripheral ADCY3–cAMP-driven regulation of adiposity and body weight may also exist in humans, and pharmacologics that affect ADCY3 activity may elicit beneficial effects in those with obesity.

Our genetic and functional human data strongly suggest that recessive pathogenic mutations in *ADCY3* cause monogenic severe obesity. Interestingly, genome-wide association studies (GWAS) have demonstrated a consistent association between frequent variants in *ADCY3* and both BMI and fat mass[19-24], reminiscent of *MC4R* and *PCSK1* where both frequent and rare DNA variants have also been linked to common and monogenic obesity, respectively[21]. Apart of its association with obesity related traits, ADCY3 has been implicated through GWAS, in other disorders including ulcerative colitis, inflammatory bowel disease and Crohn's disease [25]. Furthermore, increased methylation of sites in *ADCY3* and its promoter region have been associated with BMI[26,27]. Therefore, *ADCY3* reiterates both the genetic and epigenetic mechanisms leading to obesity that have previously been shown for *POMC*[26]. The identification of novel forms of

monogenic obesity in consanguineous families makes it imperative to screen inbred populations in our quest to identify novel pathways and physiological mechanisms leading to obesity that could remain unexposed in non-consanguineous populations.

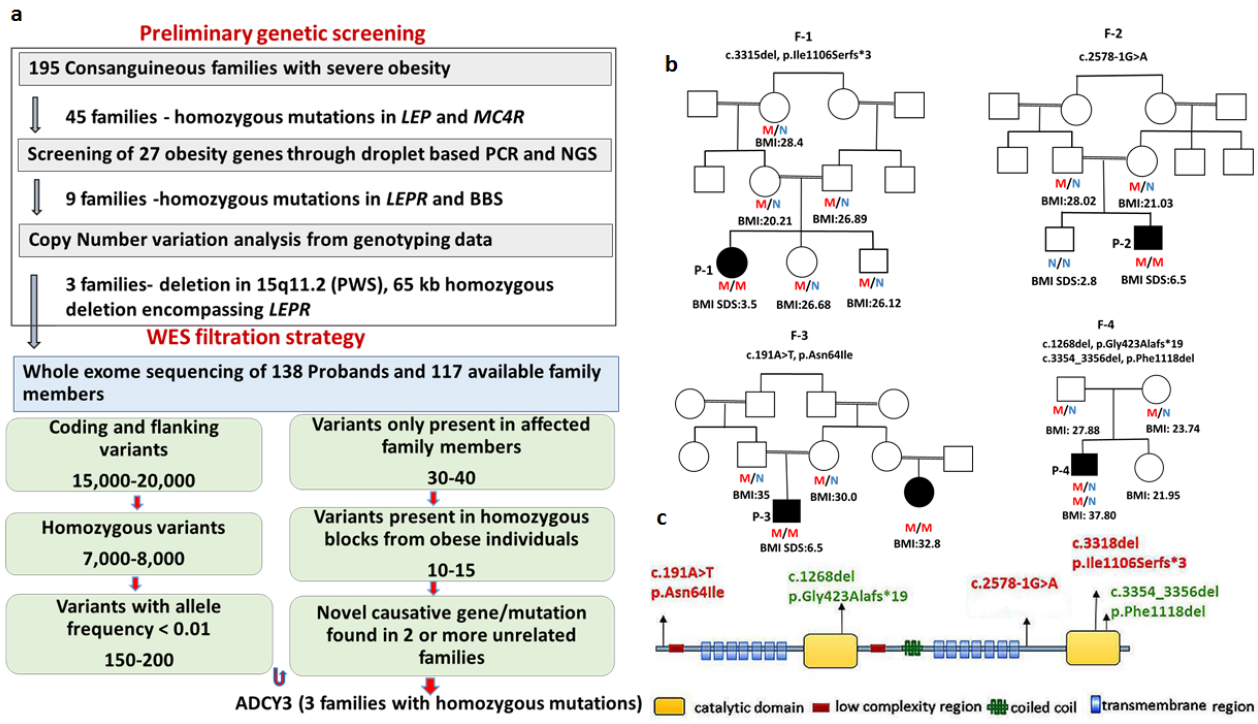

Figure 1. ***ADCY3*** **mutations identified in four affected families (a)** Schematic presentation of the stepwise genetic screening of 195 probands affected with severe obesity from a consanguineous population in Pakistan; 57 probands carried mutations in known obesity genes and were excluded from further analyses. Whole exome sequencing (WES) was performed in the remaining 138 probands and 117 family members. **(b)** Pedigrees of four affected families (Family 1-4) showing mutation status (N: normal allele; M: mutant allele) and BMI/BMI SDS. **(c)** Position of variants identified in relation to ADCY3 domains (NM_004036.4).

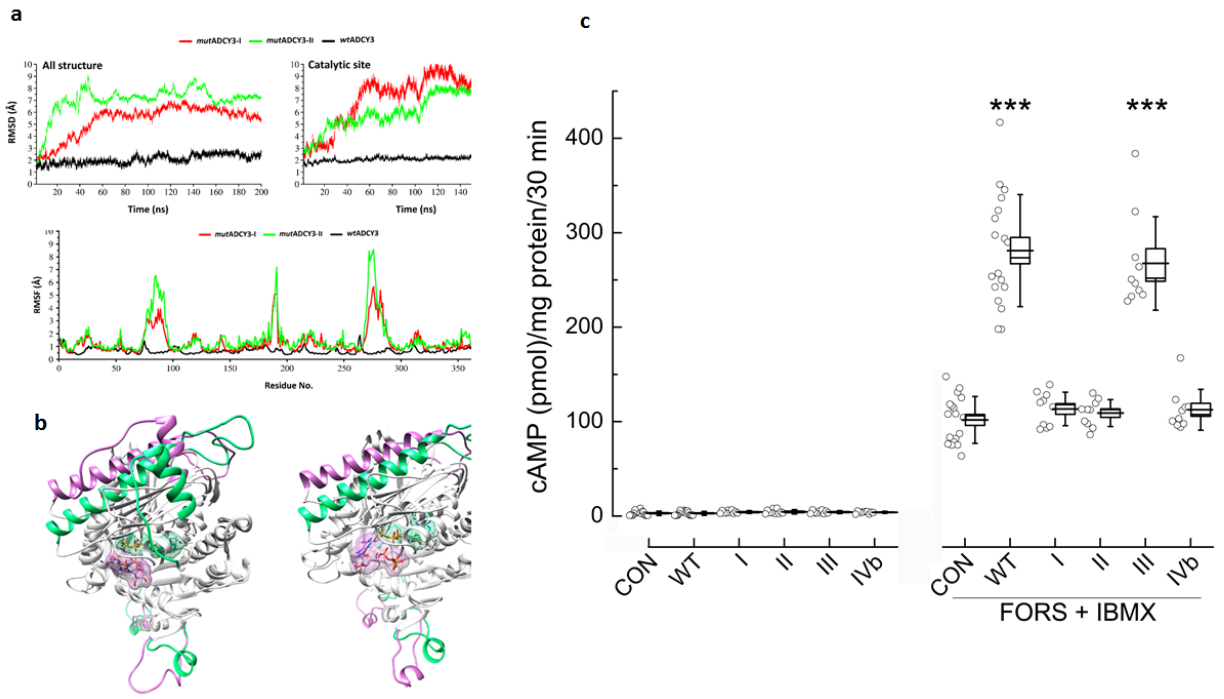

Figure 2. Effect of ADCY3 WT and mutants (a) ADCY3 backbone stability of the whole protein (left) and catalytic site (right) for *wt*ADCY3 (black), *mut*ADCY3-I (red) and *mut*ADCY3-II (green), as assessed during a 200ns molecular dynamic simulation in terms of root mean square deviation (RMSD). The mutants showed high conformational fluctuations, particularly at the catalytic site. **(b)** Residual flexibility profile for *wt*ADCY3 (black), *mut*ADCY3-I (red) and *mut*ADCY3-II (green) during 200ns molecular dynamic simulation calculated by root mean square fluctuation (RMSF) presented higher fluctuations in the ADCY3 mutants compared to the wild-type. **(c)** cAMP production in BHK cells following stimulation by Forskolin (1 µM, in the presence of 0.1 mM IBMX) for 30 min in cells transfected with pcDNA3 (control), or plasmids encoding ADCY3 (wild-type or mutant constructs). Note a significantly higher increase in human ADCY3-wt (n=18) and mutADCY3-III as compared to mutADCY3-I, mutADCY3-II, mutADCY3-IVb and control (n=8-18, given are means as horizontal bars, SD as box, SEM and individual data points; *** $p<0.001$ as compared to control, mutant I, II or IVb; ANOVA and Bonferroni post hoc test). For transient protein expression of wt and mutants, see Suppl. Figure 4. As mutADCY3-IVa is a frame-shift mutation in the catalytic domain 1 that results in a truncated protein (Fig.1b) analysis of this particular mutant was not performed.

Table 1. Physical and endocrine characteristics for the four probands with mutations in the *ADCY3* gene. Values represent mean±SEM

Characteristic	**P1**	**P2**	**P3**	**P4**
Mutation	*mutADCY3*-I*	*mutADCY3*-II	*mutADCY3*-III	*mut*ADCY3-IV a/b
Sex	Female	Male	Male	Male
Age years	15	6	6	11
Height m	1.50	1.37	1.32	1.54
Body weight kg	87	52	49	89
BMI (SDS for age)	38.7 (3.5)	28.0 (6.5)	28.1 (6.5)	37.8 (4.6)
Insulin µU/ml	48.2	10.7	13	-
Leptin ng/ml	30	22	11	-
Cortisol am µg/dl	18	11	7.5	-

Reference values from age-matched wild-type subjects from the same population (n=33): BMI (SDS for age): 17.0±1.0 (-0.4±0.1); insulin 7.2±1.0 µU/ml; leptin 3.0±0.4 ng/ml; cortisol 10.8±0.4 µg/dl (values are mean±SEM).

[1]*mutADCY3*-I: homozygous frameshift mutation (p.Ile1106Serfs*3); [2]*mutADCY3*-II: homozygous splice-shift mutation (c.2578-1G>A); [3]*mutADCY3*-III: homozygous missense mutation (p.Asn64Ile); [4]*mutADCY3*-IV a/b: compound heterozygous mutation (p.Phe1118del/p.Gly423Alafs*19).

ACKNOWLEDGEMENTS

The authors thank the patients and their families for participation in the study. We are grateful to Dr A.W. Rathore for clinical facilitation, Dr Z. Gilani for his advice regarding ADCY3 molecular modelling, M. Boissel for help with statistical analyses and Q. A. Ain and I. Qureshi for their technical assistance. This study was supported by the 'Fédération de Recherche' 3508 Labex EGID (European Genomics Institute for Diabetes; ANR-10-LABX-46), by the ANR Equipex 2010 session (ANR-10-EQPX-07-01; 'LIGAN-PM'), and by the European Community (FEDER) and the Region Hauts-de-France. The research leading to this study was also supported by funding from the European Research Council GEPIDIAB 294785 (P.F.) and the Pakistan Academy of Sciences (M.A.).

AUTHOR CONTRIBUTIONS

S.S., A.B., M.A., F.P. designed the study and wrote the first draft of the paper. S.S., Q.M.J., S.M.D., A.H. and M.A. collected samples and performed biochemical analysis. A.B., E.D., O.S. T.R., E.V., I.R., S.S and F.D.G. performed whole exome sequencing and analyzed the genetic data. J.M., H.A., D.A.S., M.A., W.I.K., T.A.B., D. and C.S. identified and recruited obese families. F.T., J.G., A.M., G.Q., R.B., A.A. and J.L. carried out the functional experiments and analysed the data. M.U.M. performed the structural analysis. All authors contributed to the final version of the manuscript.

1. El-Sayed Moustafa, J.S. & Froguel, P. From obesity genetics to the future of personalized obesity therapy. *Nat Rev Endocrinol* **9**, 402-13 (2013).
2. Froguel, P. & Blakemore, A.I. The power of the extreme in elucidating obesity. *N Engl J Med* **359**, 891-3 (2008).
3. Saeed, S. *et al.* Novel LEPR mutations in obese Pakistani children identified by PCR-based enrichment and next generation sequencing. *Obesity (Silver Spring)* **22**, 1112-7 (2014).
4. Saeed, S. *et al.* Genetic variants in LEP, LEPR, and MC4R explain 30% of severe obesity in children from a consanguineous population. *Obesity (Silver Spring)* **23**, 1687-95 (2015).
5. Saeed, S., Butt, T.A., Anwer, M., Arslan, M. & Froguel, P. High prevalence of leptin and melanocortin-4 receptor gene mutations in children with severe obesity from Pakistani consanguineous families. *Mol Genet Metab* **106**, 121-6 (2012).
6. Kopelman, P.G. Obesity as a medical problem. *Nature* **404**, 635-43 (2000).
7. WHO. A snapshot of global health. (World Health Organization, 2012).
8. Stunkard, A.J., Harris, J.R., Pedersen, N.L. & McClearn, G.E. The body-mass index of twins who have been reared apart. *N Engl J Med* **322**, 1483-7 (1990).
9. Wang, Z. *et al.* Adult type 3 adenylyl cyclase-deficient mice are obese. *PLoS One* **4**, e6979 (2009).

10. Wong, S.T. *et al.* Disruption of the type III adenylyl cyclase gene leads to peripheral and behavioral anosmia in transgenic mice. *Neuron* **27**, 487-97 (2000).
11. Cao, H., Chen, X., Yang, Y. & Storm, D.R. Disruption of type 3 adenylyl cyclase expression in the hypothalamus leads to obesity. *Integr Obes Diabetes* **2**, 225-228 (2016).
12. Pitman, J.L. *et al.* A gain-of-function mutation in adenylate cyclase 3 protects mice from diet-induced obesity. *PLoS One* **9**, e110226 (2014).
13. Hanoune, J. & Defer, N. Regulation and role of adenylyl cyclase isoforms. *Annu Rev Pharmacol Toxicol* **41**, 145-74 (2001).
14. Kanoski, S.E., Fortin, S.M., Arnold, M., Grill, H.J. & Hayes, M.R. Peripheral and central GLP-1 receptor populations mediate the anorectic effects of peripherally administered GLP-1 receptor agonists, liraglutide and exendin-4. *Endocrinology* **152**, 3103-12 (2011).
15. Liang, Y. *et al.* Hepatic adenylate cyclase 3 is upregulated by Liraglutide and subsequently plays a protective role in insulin resistance and obesity. *Nutr Diabetes* **6**, e191 (2016).
16. Ando, T. *et al.* Liraglutide as a potentially useful agent for regulating appetite in diabetic patients with hypothalamic hyperphagia and obesity. *Intern Med* **53**, 1791-5 (2014).
17. Madsen, L. & Kristiansen, K. The importance of dietary modulation of cAMP and insulin signaling in adipose tissue and the development of obesity. *Ann N Y Acad Sci* **1190**, 1-14 (2010).
18. Tong, T., Shen, Y., Lee, H.W., Yu, R. & Park, T. Adenylyl cyclase 3 haploinsufficiency confers susceptibility to diet-induced obesity and insulin resistance in mice. *Sci Rep* **6**, 34179 (2016).
19. Warrington, N.M. *et al.* A genome-wide association study of body mass index across early life and childhood. *Int J Epidemiol* **44**, 700-12 (2015).
20. Speliotes, E.K. *et al.* Association analyses of 249,796 individuals reveal 18 new loci associated with body mass index. *Nat Genet* **42**, 937-48 (2010).
21. Wen, W. *et al.* Meta-analysis identifies common variants associated with body mass index in east Asians. *Nat Genet* **44**, 307-11 (2012).
22. Monda, K.L. *et al.* A meta-analysis identifies new loci associated with body mass index in individuals of African ancestry. *Nat Genet* **45**, 690-6 (2013).
23. Stergiakouli, E. *et al.* Genome-wide association study of height-adjusted BMI in childhood identifies functional variant in ADCY3. *Obesity (Silver Spring)* **22**, 2252-9 (2014).
24. Felix, J.F. *et al.* Genome-wide association analysis identifies three new susceptibility loci for childhood body mass index. *Hum Mol Genet* **25**, 389-403 (2016).
25. Liu, J.Z. *et al.* Association analyses identify 38 susceptibility loci for inflammatory bowel disease and highlight shared genetic risk across populations. *Nat Genet* **47**, 979-986 (2015).
26. Voisin, S. *et al.* Many obesity-associated SNPs strongly associate with DNA methylation changes at proximal promoters and enhancers. *Genome Med* **7**, 103 (2015).

ONLINE METHODS

Study subjects. The 138 probands included in this study are part of our initial cohort comprising 195 unrelated probands presenting severe obesity of early onset (before 6 years of age). Severe obesity was defined by a BMI SDS $\geq$ 3. The subjects were recruited from public hospitals in the central province of Punjab, Pakistan, following the patient/parent written informed consent. The study protocol was approved by the ethics/research committees of Children's Hospital and the University of Lahore, Lahore, Pakistan. Consent to publish photos was obtained in all patients c. Probands and/or their parents were interviewed to obtain family and medical history and family pedigrees spanning at least three generations were constructed. As a rule, in case of identification of a homozygous variant suspected of its association with obesity, other members of the affected family were invited to participate in the study, subject to their availability and consent. Clinical cases of syndromic obesity were excluded from the study. Anthropomorphic measurements and physical examination were carried out and blood samples were obtained in each case for subsequent DNA extraction and biochemical analyses. The single European/American case included in the present study, was referred to the out-patient clinic in Maastricht University Medical Center to establish the genetic cause of obesity. After receiving genetic counselling the parents provided written consent to participate in the study.

Smell test. Smell testing of probands from Pakistan and their family members was performed at the ENT unit of the Children's Hospital Lahore. Preceding the test for a possible loss of ability to smell, the subject was thoroughly examined for upper respiratory infections, rhinitis, chronic sinusitis or presence of nasal masses such as polyps. A semi-quantitative test was administered to assess smell function based on the patient's response to 3 different sniff odorants each at four serial dilutions presented in a random sequence. The subjects were blindfolded before testing. The test was scored (0-12) on the subject's correct responses. The individual scores reflected the extent of loss of olfactory function (normosmia: 10-12; mild to moderate microsmia: 5-9; acute microsmia: 3-4; anosmia: 0-2). No adjustments were made for age or sex. The European/American proband with compound heterozygous mutation was not tested for sense of smell but was reported to have no sense of smell.

Preliminary genetic screening. All probands (except the European/American case) were primarily screened for pathogenic mutations in the coding exons of *LEP* and *MC4R* by conventional sequencing. A further 27 known genes associated with non-syndromic and syndromic obesity, were analysed using one-step PCR based microdroplet enrichment (RainDance Technologies) followed by next-generation sequencing (NGS) as previously described[3] **(Fig. 1a).** Additionally, genome-wide genotyping was performed to find structural variants in obesity associated genes. These screening procedures identified 57 probands with homozygous loss-of-function mutations in known obesity-associated genes (published[3-5] and unpublished data).

Whole exome sequencing (WES) and data analysis. Genomic DNA samples from the remaining 138 probands and their available family members were processed using the Agilent SureSelectXT Human All Exon Kit (version V5+UTRs; Agilent Technologies) or the NimbleGen SeqCap EZ MedExome Target Enrichment kit (Roche NimbleGen), following the manufacturer's protocol. The first group of 96 samples processed through Agilent protocol, were sequenced using Illumina HiSeq 2500 (Illumina) with 100 bp paired-end reads, whereas the second group of 159 samples processed through NimbleGen protocol were sequenced using Illumina HiSeq 4000 (Illumina) with 150 bp paired-end reads. The demultiplexing of sequence data was performed with bcl2fastq2 Conversion Software (Illumina). Subsequently, sequence reads from FASTQ files were mapped to the human genome (hg19/GRC37) using the Burrows-Wheeler Aligner and a local realignment was processed using GATK. Variant calling was performed using GATK HaplotypeCaller (ref or URL). Only genotypes with sequencing depth of $> 8\times$ were selected for further analyses. The variant annotation was performed using the Ensembl Perl API and other Perl scripts to include data from dbSNP and dbNSFP. All DNA samples were sequenced with an average read depth of $>80\times$.

For the European/American child, WES was performed in the index patient and both parents (trio approach). Exome capture was carried out using the Agilent SureSelect Human All Exon enrichment kit (Agilent Technologies). Sequencing was performed on an Illumina HiSeq platform (BGI, Copenhagen, Denmark). The data were analysed with BWA (read alignment) and GATK (variant calling) software packages and the variants were annotated using an in-house developed pipeline.

Variant prioritisation and candidate gene discovery. Autosomal recessive homozygosity for disease-associated mutation(s) was expected in all probands with consanguineous parentage. To identify candidate genes and/or mutations associated with obesity, variations in each family were

filtered individually to detect potentially causative homozygous mutations in affected individuals. In the initial filtration step, all heterozygous variants present in obese individuals were removed. As the likelihood of any novel causative or deleterious variant annotated in publically available databases is low, variants with an allele frequency of ≤0.01% in the 1000 Genomes Project database, Exome Variant Server (EVS) and ExAC (Exome Aggregation Consortium) were excluded. Finally, any homozygous variants in family members exhibiting a normal body weight (BMI< 28) were excluded from further analysis. Polyphen and MutationTaster *in silico* mutation prediction software were used to predict pathogenicity. Variants that were synonymous were also removed from further analyses. Potentially deleterious mutations present in regions of homozygosity (ROH) were given priority for further analysis. Using this approach **(Fig. 1a**), an average of ~16,000 high quality variants were initially identified per individual from paired end reads that after filtering came down to 10-15 variants (Supplementary Table 5,6 and 7). Genes identified in ≥2 families were considered candidates for obesity. Following these sequential steps, we identified *ADCY3* as a valid candidate gene for obesity.

As a first step, the European/American proband was screened against a diagnostic Kallmann syndrome/hypogonadotrophic hypogonadism (KS/HH) gene panel that included 26 genes associated with KS/HH. No potentially pathogenic 'de novo', homozygous, compound heterozygous or X-linked variants were detected in the coding or splice-site regions of these 26 genes through filtering steps using ESP dbSNP and in-house databases, and dbSNP at a frequency level of <1%. Because of the negative results obtained with the KS/HH panel we continued by using a stringent filtering regimen for the rest of the variants. This involved filtering for <5% in dbSNP, <1% in the in-house database and >3.5% in phyloP for variants located in coding regions and splice sites. The filtration reduced the number of variants to 109. By filtering for de novo, homozygous or compound heterozygous variants only three variants were identified (Supplementary Table 8). Of these variants, the *ADCY3* compound heterozygous variants were of most interest as these corroborated well with the patient's phenotype.

Mutations identified in *ADCY3*. The mutations identified in consanguineous families included a homozygous frameshift mutation c.3315del; p.Ile1106Serfs*3 (*mutADCY3*-I). This mutation in the last exon (coding exon 21) of the *ADCY3* gene **(Fig. 1c; Supplementary fig. 2)** results in a truncated protein by introducing a stop codon after two aberrant amino acids. The second variant, c.2578-1G>A (*mutADCY3*-II) was identified as a splice-site mutation. Here, the nucleotide substitution abolished the essential splice acceptor site at intron 15 as predicted by the Human

Splicing Finder **(Supplementary Note 1**). As a result of exon skipping, the mutated protein consists of only 1091 amino acids instead of the usual 1144 amino acids. The third homozygous variant, c.191A>T; p Asn64Ile ((*mutADCY3*-III) was a missense mutation. The fourth mutation was identified in a non-consanguineous European/American family is a compound heterozygous mutation c.1268del; p.Gly423Alafs*19 (*mutADCY3*-IVa) and c.3354_3356del; p.Phe1118del (*mutADCY3*-IVb).

Polymerase chain reaction (PCR), sequencing and mutational analysis. Mutations identified in *ADCY3* gene through WES were confirmed in the probands and their family members by standard PCR and Sanger sequencing using a 3730 DNA analyser (Life Technologies) in the probands and their family members. Sequence traces were analysed using the Mutation Surveyor software package (SoftGenetics). The PCR primers and theromocycler conditions are available in **Supplementary Table 4**.

***ADCY3* expression analysis.** Two ml of blood was drawn in PAXgene Blood RNA tubes and RNA was extracted using the PAXgene RNA Blood kit (Qiagen) according to the manufacturer's instructions. *ADCY3* gene expression was analysed for P1 (*mutADCY3*-I homozygote) and a family member (*mutADCY3*-I heterozygote) by quantitative reverse transcription PCR (RT-PCR). Briefly, 300-500 ng of total RNA was converted to cDNA using the High Capacity RNA-to-cDNA Kit (Life Technology) in a final reaction of 20 µl. Gene expression was performed by TaqMan assay (Life Technologies) using the following primers: hADCY3 FAM (Hs01086502_m1) and internal control housekeeping gene B2M VIC (Hs00984230_m1). All quantitative PCR reactions were set up in triplicate in a 384-well plate (Life Technologies). Each well contained 1 µl of cDNA (diluted 1:3) and 9 µl of the reaction mix, that is, 5 µl of TaqMan Gene Expression Mix (cat no. 4370048, Life Technologies), 0.5 µl of target and control probes and 3µl of nuclease-free water, making a total reaction volume of 10 µl. The qPCR was performed using the 7900HT Fast Real-Time PCR System (Life Technologies). The 2^{-DDCT} method was used to quantify the level of ADCY3 in both samples against a standard control.

Whole genome genotyping. Genome-wide high-density genotyping was performed by using the HumanOmni 2.5S BeadChip KIT (Illumina) containing >$2.5x10^6$ variants with a minor allele frequency (MAF) of 2.5%, according to the manufacturer's instructions. A genotyping project was created in GenomeStudio using the standard cluster file and the genotypes were assigned to each SNP based on the flourescent intensity data. A reproducibility and heritability report was generated to ensure that the parent-to-child heritability frequency (P-C Heritability Freq) was

≥0.99. Finally, the cluster file was exported and reports were generated for subsequent calling of ROH.

Detection of Runs of Homozygosity (ROH): ROH was detected using the plink open source whole genome association analysis toolset, to identify an autozygous region in the affected inbred individuals. The genotyping data were subjected to quality control to remove individuals missing >5% genotype data, excluding SNPs with a MAF≤0.05, markers that failed to comply with a Hardy-Weinberg threshold of 0.001 and individuals and/or markers on the basis of Mendelian error rate (ME).

Biochemical determinations. Serum hormone concentrations were measured in duplicate by enzyme-linked immunosorbent assay (ELISA) using commercially available kits (insulin and cortisol: Monobind; leptin: Organium Laboratories), with an EIA analyser (Bio-Rad Laboratories). Samples were analysed according to the manufacturer's instructions. The inter-assay and intra-assay variations were <10%. All other biochemical analytes (blood glucose, serum triglycerides, cholesterol, LDL-C, HDL-C; hsCRP, 25-hydroxy vitamin-D, creatinine and blood urea nitrogen) were determined by chemiluminescence assay (CHEMIFLEX). Fasting blood glucose and insulin levels were used to measure homeostasis model assessment of insulin resistance (HOMA-IR).

Molecular Modelling. Stepwise molecular modelling was performed to determine the structural consequences of the mutations identified in the *ADCY3*. Briefly, homology modelling of wild-type ADCY3 (*wt*ADCY3) and its different mutated forms (*mut*ADCY3) was coupled with a molecular dynamics (MD) simulations for model refinement. Molecular docking of Mg-ATP molecule on the catalytic site followed by a long run MD simulation of the docked complex was carried out to assess the stability of the ADCY3 backbone in its mutated forms **(Supplementary Fig. 8, Supplementary Fig. 9).** In this study *mutADCY3*-I (p.Ile1106Serfs*3, translating a shorter sequence of 1108, instead of 1144, after two aberrant amino acids, serine and leucine) and *mutADCY3*-II (c.2578-1G>A, translating a sequence of 1091aa instead of 1144) were used for homology modelling along as compared to *wt*ADCY3. In the case of compound heterozygous mutation, *mutADCY3*-Iva and b (p.Gly423fs*19 and p.Phe1118del), the first mutation occurs in the C1 catalytic domain and causes the translation of 18 aberrant amino acids followed by a premature stop codon. Consequently, native folding of this protein is predicted to fail due to a marked truncation of the catalytic domain and the protein is likely to assume an unpredictable conformation that may lead to a loss of function. Modelling of the truncated domain conformation was not possible due to a lack of known structural information in the Protein Data Bank (PDB).

Further analysis of the *wt*ADCY3 structure showed that the amino acids lacking in p.Gly423fs*19 are normally involved in the interaction with Mg-ATP, the C2 catalytic domain and G□s and correct conformation of this region of the protein is necessary for normal function. Homology models of *wt*ADCY3 and *mut*ADCY3 were refined by MD simulations to further elucidate molecular docking with Mg-ATP. AutoDock Vina[28] was used to study the predicted docked conformations of ADCY3 with ATP and the binding affinity of ATP-mg at the catalytic interface in *wt*ADCY3 and *mut*ADCY3. Assessment of ATP-Mg docking at the interface of both ADCY3 catalytic domains, where cAMP is catalyzed in response to G-protein signaling, was performed as described (see **Supplementary Note 2**). To further investigate the stability of docked complexes, a production simulations run of 200ns at 300K and I bar pressure in explicit solvation model (with TIP3P water module) was performed in each case after a stepwise minimization and equilibration. AMBER 16 simulation package (Case et al., 2012) was employed throughout for all simulations (see **Supplemetary Notes 2** for detailed protocol).

Generation of wild-type and mutant ADCY3 expression constructs. Full-length *ADCY3* was amplified from a human *ADCY3* cDNA clone (NM_004036, cat.no. RC220272; Origene, Maryland, USA) using Q5 High-Fidelity DNA polymerase (New England BioLabs, Massachusetts, USA). The forward (5'-ATCATCGGCGCGCC AATGCCGAGGAACCAGGGCTTCTC-3') and reverse (5'-ATCATCGCGGCCGCTCAGGAGTTGTCCACCACCTGGTG -3') primers included restriction sites (underlined) for AscI and NotI, respectively. The resulting 3.4 kb PCR fragment was verified by gel electrophoresis, digested with AscI and NotI, and column-purified. The AscI–NotI *ADCY3* gene was then cloned into the polylinker of the pCMV6-AN-Myc mammalian expression vector that contains an N-terminus Myc tag (Origene, cat. no. PS100012). The ligated plasmid was transformed in DH5 Alpha competent cells (Invitrogen, California, USA), plated onto 50 ug/ml ampicillin agar plates and individual colonies were analysed after 24 h growth at 37^{o}C. The resulting wild-type plasmid (Myc-hADCY3wt) was verified by sequencing. The four identified *ADCY3* mutations (*mutADCY3*-I, *mutADCY3*-II, *mutADCY3*-III and *mutADCY3*-IVb) were introduced into the Myc-hADCY3wt plasmid by site directed mutagenesis using the Q5 Site-Direct Mutagenesis kit (New England Biolabs). Primers for mutagenesis were designed according to the manufacturer's recommendations and the sequences (5'–3') are given in **Supplementary Table 9**. The amplified products were transformed into DH5 alpha cells as described above, and the plasmid sequences were again verified by sequencing before functional analyses. pcDNA3 without any inserted DNA sequence was used as the control plasmid in cellular assays.

Cell culture and transient transfection. Chinese hamster ovary (CHO cells were maintained in 1:1 DMEM/F12 culture medium (Thermo Fisher Scientific Inc) supplemented with 10% fetal calf serum (FCS) and 1% penicillin/streptomycin mixture (Sigma-Aldrich). Baby hamster kidney (BHK) cells (ATCC) were maintained in BHK medium (DMEM, 10% FCS, 10 mM HEPES, 2 mM glutamine) in a humidified incubator at 37°C with 5% CO_2. Cells were passaged by trypsinisation every 3 days. A total of 3,000 BHK cells/well were seeded in 24-well plates (Nalge Nunc International) with or without 18 mm-diameter glass cover slips and cultured in BHK medium. After 72 h, cells were transfected with 500 ng of the indicated plasmids using 0.5 µl jetPEI® (Polyplus, Illkirchen, France) in 1.1 ml BHK medium. After 72 h, the wells were washed with PBS prior to further analysis.

Western blotting. For Western blotting, cells were detached in PBS containing 10 mM EDTA at 37°C, centrifuged and pellets resuspended in Laemmli's sample buffer followed by brief sonication. Samples were separated by SDS-PAGE (10% gel) and subsequent immunoblotting was performed using rabbit anti-Myc antibodies (1:3000; Sigma, C3956)) or anti-ADCY3 (raised against the extracellular domain; 1:1000; Alomone Labs, Jerusalem, Israel) as previously described[29]. Secondary antibodies (HRP-coupled donkey anti-rabbit; GE Healthcare) were used at a 1:3000 dilution and binding detected by ECL Proteins were detected by Ponceau's stain and all blots were imaged using FLUORCHEM 8000 (Alpha Innochem).

Immunocytochemistry. Cells on coverslips were washed in PBS, fixed with 4% paraformaldehyde in PBS, permeabilised with 2% saponin and incubated with antibodies, as previously described[29]. The antibodies, rabbit anti-myc (1:300; Sigma, C3956) and anti-Adcy3 (Alomone Labs), were used at a dilution of 1:100. The secondary antibodies were used at a 1:3000 dilution (Cy3 donkey anti-rabbit, Jackson ImmunoResearch). Confocal analysis was performed as previously described[29] using a Zeiss LSM 510 meta-confocal microscope (Zeiss, Göttingen, Germany) with an ApoPLAN ×63 objective.

cAMP assay. Levels of cAMP production were determined at 37°C in BHK cells that were transfected with pcDNA3, myc-tagged hADCY3wt or hADCY3-mutant plasmids. Cells were washed in Krebs-Ringer buffer (KRB, in mM) (135 NaCl, 3.6 KCl, 5 $NaHCO_3$, 0.5 NaH_2PO_4, 0.5 $MgCl_2$, 10 HEPES, 1.5 $CaCl_2$, 5 glucose, in 0.1% BSA; pH 7,4) and subsequently incubated for 30 min in KRB in the presence or absence of 2 µM forskolin and 0.1 mM IBMX[30]. Following incubation, KRB was aspirated and the cells were solubilized with 0.1 M HCl/1% Triton X-100 solution (300 µl/well) at 37° C for 30 min. The cell solution was centrifuged at 600x*g* for 5 min, at 4°C, and the supernatants were either stored at -80°C or assayed directly using the Cyclic AMP

Direct EIA Kit (Arbor Assays). Total protein content of the supernatants was determined by bicinchoninic acid assay (Thermofisher).

Luciferase activity. The CHO cells ($1x10^5$) plated in 96-well dishes were transiently transfected with 1 µg of plasmid including 400 ng of CreLuc reporter[31] with 50 ng pCMV-betaGal (for normalization) plus 100 ng of myc-tagged hADCY3wt or hADCY3-mutant plasmids or or the empty vector, using the FuGENE® 6 transfection reagent (Promega) according to the manufacturer's protocol. After transfection (44 hours) the cells were incubated with fresh medium supplemented with 2% FCS and 100 µM IBMX plus 1 µM forskolin or DMSO (vehicle) for 4 hours. The cells were then washed with PBS and lysed using Passive lysis Buffer (Promega). O-nitrophenyl-β-D-galactopyranoside (ONPG) was used as the substrate for β-galactosidase and activity was measured with a microplate reader at absorbance 450 nm. Luciferase activities were measured with 25 µl of protein extracts solution by using the Luciferase reporter assay system (Promega) according to the manufacturer's protocol. Luciferase activity was calculated as relative luminescence units (RLU) normalized against β-galactosidase activity.

URLs. ExAC browser, http://exac.broadinstitute.org/; UCSC Genome Browser, http://genome.ucsc.edu/; PolyPhen-2, http://genetics. bwh.harvard.edu/pph2/index.shtml;Exome Variant Server, http://evs.gs.washington.edu/EVS/; Human splicing finder. http://www.umd.be/HSF/; Plink. http://zzz.bwh.harvard.edu/plink/download.shtml; SoftGenetics, http://www.softgenetics.com/mutationSurveyor.php, GATK,https://software.broadinstitute.org/gatk/documentation/tooldocs/current/org_broadinstitute_gatk_tools_walkers_haplotypecaller_HaplotypeCaller.php

Data availability. The sequencing data (FASTQ files) of the probands with *ADCY3* mutation included in this study have been deposited in the NCBI Sequence Read Archive database under Accession Number SAMN07490276 (F1, mut I), SAMN07490319 (F2, mut II), SAMN07490318 (F3, mut III).

27. Liu, X. *et al.* Maternal preconception body mass index and offspring cord blood DNA methylation: exploration of early life origins of disease. *Environ Mol Mutagen* **55**, 223-30 (2014).
28. Trott, O. & Olson, A.J. AutoDock Vina: improving the speed and accuracy of docking with a new scoring function, efficient optimization, and multithreading. *J Comput Chem* **31**, 455-61 (2010).
29. Boal, F., Laguerre, M., Milochau, A., Lang, J. & Scotti, P.A. A charged prominence in the linker domain of the cysteine-string protein Cspalpha mediates its regulated interaction with the calcium sensor synaptotagmin 9 during exocytosis. *FASEB J* **25**, 132-43 (2011).

30. Roger, B. *et al.* Adenylyl cyclase 8 is central to glucagon-like peptide 1 signalling and effects of chronically elevated glucose in rat and human pancreatic beta cells. *Diabetologia* **54**, 390-402 (2011).
31. Ferdaoussi, M. *et al.* Exendin-4 protects beta-cells from interleukin-1 beta-induced apoptosis by interfering with the c-Jun NH2-terminal kinase pathway. *Diabetes* **57**, 1205-15 (2008).